

Role of ataxia-telangiectasia mutated in hydrogen peroxide preconditioning against oxidative stress in Neuro-2a cells

JIANHUA WU^{1*}, FANG WANG^{1*}, ZHIQIANG SU², JUE LIU³,
SANG HU¹, HAO LI¹, PEI HU¹ and DONGFANG WU¹

¹Department of Pharmacy, Zhongnan Hospital of Wuhan University, Wuhan, Hubei 430071;

²Department of Pharmacy, The First Affiliated Hospital of Guangzhou University of Traditional Chinese Medicine, Guangzhou, Guangdong 510405; ³Department of Pharmacy, The Central Hospital of Wuhan, Tongji Medical College, Huazhong University of Science and Technology, Wuhan, Hubei 430014, P.R. China

Received December 16, 2015; Accepted January 27, 2017

DOI: 10.3892/mmr.2017.6510

Abstract. Ischemic preconditioning is an endogenous protective mechanism that may be triggered by exposure to hydrogen peroxide (H₂O₂). However, the exact mechanisms underlying preconditioning remain to be fully understood. Ataxia-telangiectasia mutated (ATM) is regarded as an essential endogenous protective protein against stress. The aim of the present study was therefore to investigate whether ATM mediates H₂O₂ preconditioning. Preconditioning of Neuro-2a (N2a) cells with 100 μ M H₂O₂ for 90 min resulted in protection from injury induced by a long period of exposure to 600 μ M H₂O₂. In addition, preconditioning with 100 μ M H₂O₂ activated ATM and increased ATM mRNA and protein expression levels in N2a cells. Furthermore, the protective effects induced by H₂O₂ preconditioning were attenuated by pretreatment with the ATM inhibitor, Ku55933, or ATM small interfering RNA. In conclusion, these findings suggested that ATM is involved in H₂O₂ preconditioning-mediated protection against oxidative stress-induced injury in N2a cells. To the best of our knowledge, the present study demonstrated, for the first time, that the ATM protein is a key mediator of H₂O₂ preconditioning.

Introduction

Ischemic preconditioning is an endogenous protective mechanism whereby tissue subject to single or multiple brief episodes of ischemia/reperfusion develops protection against

subsequent potentially lethal ischemic injury. Previous studies have demonstrated that preconditioning is additionally triggered by non-ischemic stress, including exposure to reactive oxygen species (ROS) (1,2). However, the exact mechanisms underlying preconditioning remain to be fully understood.

Ataxia-telangiectasia mutated (ATM) serine/threonine kinase is a member of a superfamily of phosphatidylinositol (PI) 3-kinase-like kinases (3) and is regarded as a lynchpin of cellular defenses to stress, particularly antioxidative stress, maintaining cellular redox homeostasis (4). Previous studies have reported that ATM-deficient mice have increased levels of ROS, particularly in the nervous system, leading to neuronal degeneration (5,6). In addition, it has been reported that activation of ATM in the cytoplasm protects neurons against oxidative stress-induced damage (7). Patients with ataxia telangiectasia, carrying mutations at the two ATM alleles (ATM^{-/-}), present with progressive cerebellar ataxia and cerebellar degeneration (8,9). There is accumulating evidence to suggest that ATM is a central regulator of the response to DNA damage, including DNA repair, telomere maintenance and regulation of the cell cycle (10-12). Although ATM is expressed in the brain and neurons (13), its involvement in preconditioning remains to be investigated. The present study investigated whether H₂O₂ preconditioning protected against injury induced by oxidative stress in Neuro-2a (N2a) cells, and the role of ATM in H₂O₂ preconditioning.

Materials and methods

Cell culture and treatment. N2a mouse neuroblast cells (Sigma-Aldrich; Merck KGaA, Darmstadt, Germany) were cultured in high-Dulbecco's modified Eagle's medium/OPTI-Minimal Essential Medium (1:1; Gibco; Thermo Fisher Scientific, Inc., Waltham, MA, USA) containing 5% (v/v) fetal bovine serum (Gibco; Thermo Fisher Scientific, Inc.) in a humidified atmosphere of 5% CO₂ at 37°C. Cells were passaged by trypsinization and seeded at $\sim 10^5$ cells/ml. When cells reached 60-80% confluence, the culture medium was replaced with serum-free medium for 12-24 h. Cells were initially treated with 20, 50, 100, 300, 600 and 1,000 μ M H₂O₂ for 12 h to assess the effect of different doses of H₂O₂ on

Correspondence to: Professor Dongfang Wu, Department of Pharmacy, Zhongnan Hospital of Wuhan University, 169 Dong-Hu Road, Wuhan, Hubei 430071, P.R. China
E-mail: dfwu2010@whu.edu.cn

*Contributed equally

Key words: ataxia-telangiectasia mutated, preconditioning, hydrogen peroxide

N2a cell viability. The results of this treatment indicated that 600 μM H_2O_2 was the median lethal dose. Therefore, 600 μM H_2O_2 was used for subsequent experiments. Subsequently, cells were pretreated with 100 μM H_2O_2 for 90 min followed by 12 h recovery and subsequent exposure to the median lethal dose of 600 μM H_2O_2 for 12 h. To evaluate the involvement of ATM in preconditioning-induced protection, additional experiments were performed. N2a cells were treated with 10 μM ATM-specific inhibitor Ku55933 (Sigma-Aldrich; Merck KGaA) for 30 min or transfected with ATM small interfering RNA (siRNA) for 36 h prior to H_2O_2 preconditioning. Following H_2O_2 preconditioning, these cells were subjected to the lethal dose of 600 μM H_2O_2 .

Assessment of cell viability. An MTT assay was used to determine cell viability. N2a cells were seeded at a density of 1×10^4 cells/well in a 96-well culture plate. At the end of each experiment, 10 μl MTT (0.5 mg/ml) was added to the cell medium and incubated for 4 h at 37°C. Following incubation, MTT solutions were removed, dimethyl sulfoxide was added, and the absorbance at 490 nm was measured using a microplate reader. Data are expressed as a percentage of the control, which was considered to be 100% viable.

siRNA transfection. N2a cells were transfected with 50 nM ATM siRNA or Scramble control siRNA using Lipofectamine 2000® reagent (Invitrogen; Thermo Fisher Scientific, Inc.), according to the manufacturer's protocol. The siRNA sequences utilized targeted the following mouse ATM coding sequence: 5'-GCTTGAGGCTGATCCATATTC-3'. To determine the effect of siRNA transfection, the N2a cells were collected and lysed with lysis buffer [50 mM NaCl, 10 mM Tris-base, 1 mM EDTA, 2 mM sodium orthovanadate (Na_3VO_4), 1 mM NaF, 1 mM phenylmethyl-sulfonyl fluoride, 1% sodium dodecyl sulfate (SDS)] at 95°C for 10 min for western blot analysis 48 h following transfection.

RT-qPCR. Total cellular RNA was isolated using TRIzol® reagent (Invitrogen; Thermo Fisher Scientific, Inc.) and cDNA was generated from 1 μg total RNA using the M-MLV reverse transcription kit (Promega Corporation, Madison, WI, USA). Quantification of gene copies was performed using the ABI 7300 Real-Time PCR system (Applied Biosystems; Thermo Fisher Scientific, Inc.) with the Power SYBR® Green PCR Master Mix kit (Promega Corporation). The primer sequences used were as follows: Forward, 5'-GCACACGGATTGCTC AAGGA-3' and reverse, 5'-GCCCATTCGGAATATGGA TCAG-3' for ATM (14); and forward, 5'-CAATGACCCCTT CATTGA-3' and reverse, 5'-GACAAGCTTCCCGTTCTC AG-3' for GAPDH (15). The following thermocycling conditions were used: An initial predenaturation step at 95°C for 10 min, followed by 40 cycles of denaturation at 95°C for 15 sec and annealing at 60°C for 60 sec. All amplification reactions for each sample were repeated in at least triplicate, and the relative expression values were normalized to those of GAPDH using the $2^{-\Delta\Delta C_q}$ method (16).

Western blot analysis. Cells were lysed with lysis buffer [50 mM NaCl, 10 mM Tris-base, 1 mM EDTA, 2 mM Na_3VO_4 , 1 mM NaF, 1 mM phenylmethyl-sulfonyl fluoride, 1% SDS],

and the protein content of the lysates was measured using the bicinchoninic acid assay. Subsequently, 40 μg /lane protein was separated by 7.0% SDS-polyacrylamide gel electrophoresis and electrophoretically transferred to a nitrocellulose membrane. The membranes were blocked with 5% bovine serum albumin (Beyotime Institute of Biotechnology, Haimen, China) in TBS containing 1% Tween 20 at room temperature for 1 h, and incubated with ATM (mouse monoclonal antibody; dilution, 1:1,000; cat. no. sc-47739; Santa Cruz Biotechnology, Inc., Dallas, TX, USA), phosphorylated (p)-ATM antibodies (mouse monoclonal antibody; dilution, 1:500; cat. no. sc-73615; Santa Cruz Biotechnology, Inc.) and β -actin (rabbit polyclonal antibody; dilution, 1:1,000; cat. no. sc-130656; Santa Cruz Biotechnology, Inc.) at 4°C overnight, followed by incubation with a horseradish peroxidase-conjugated secondary antibody (either goat anti-rabbit; dilution, 1:1,000; cat. no. A0208. Or goat anti-mouse; dilution, 1:1,000; cat. no. A0216; Beyotime Institute of Biotechnology) for 1 h at room temperature. The immunostaining was visualized by enhanced chemiluminescence (Beyotime Institute of Biotechnology). The blots were scanned, and the pixel count and intensity of each band was quantified using the Scion Image software (version 4.2.3.2; Scion Corporation, Frederick, MD, USA). The results were normalized to β -actin expression.

Flow cytometric analysis of apoptosis. Flow cytometry was performed as described in a previous study by Tang *et al.* (1). Briefly, treated N2a cells (2×10^6) were collected and centrifuged at 5,000 $\times g$ at 4°C for 10 min. The cell pellet was resuspended in cold PBS and fixed using 70% ethanol at 4°C for 1 h. The cells were then centrifuged at 5,000 $\times g$ for 10 min, and resuspended in PBS. DNase-free RNaseA (100 μl , 200 $\mu\text{g}/\text{ml}$) was added to the cells and incubated at 37°C for 10 min. Cells were subsequently incubated with propidium iodide (PI) at a final concentration of 100 mg/l, filtered and incubated in the dark at room temperature for 10 min prior to flow cytometric analysis. The PI fluorescence of individual nuclei was measured using a flow cytometer (Beckman-Coulter, Inc., Brea, CA, USA). DNA labeling data were analyzed using CellQuest v.3.0 sampling software (BD Biosciences, Franklin, NJ, USA) for flow cytometry.

Caspase-3 activity assay. Caspase-3 activity was measured using a colorimetric CaspACE kit (Promega Corporation) according to the manufacturer's protocol. Cells were lysed using the kit lysis buffer (Promega Corporation) and centrifuged for 5 min at 5,000 $\times g$ and 4°C. The supernatant was used for the measurement of caspase-3 activity.

Determination of 8-hydroxy-2'-deoxyguanosine (8-OHdG) in DNA. DNA was extracted from N2a cells with the DNA Extractor kit (Wako Pure Chemical Industries, Ltd., Osaka, Japan) according to the manufacturer's protocol. The extracted DNA was digested with 8 units nuclease P1 (Cell Biolabs, Inc., San Diego, CA, USA) for 2 h at 37°C in a final concentration of 20 mM sodium acetate (pH 5.2), followed by treatment of 6 units alkaline phosphatase for 1 h at 37°C in a final concentration of 100 mM Tris (pH 7.5). The reaction mixture was centrifuged for 5 min at 6,000 $\times g$ and 4°C, and the supernatant was used for the 8-OHdG Quantitation ELISA assay (catalog

no. STA-320; Cell Biolabs, Inc.), according to the manufacturer's protocol.

Statistical analysis. SPSS statistical software was used for statistical analysis (version 18.0; SPSS, Inc., Chicago, IL, USA). The data are expressed as the mean \pm standard error of at least 3 replicate experiments. Comparisons among multiple groups were performed using one-way analysis of variance followed by the Student-Newman-Keuls post hoc test. $P < 0.05$ was considered to indicate a statistically significant difference.

Results

Effect of H_2O_2 preconditioning on cell viability following oxidative stress. The effect of different concentrations of H_2O_2 on N2a cell viability was evaluated by MTT assay (Fig. 1). Treatment with 20–100 μM H_2O_2 did not significantly affect N2a cell viability; however, concentrations of 300, 600 and 1,000 μM significantly decreased N2a cell viability compared with the control, to 78.5 ± 6.5 ($P < 0.05$), 44.2 ± 3.5 ($P < 0.01$) and $11.4 \pm 1.4\%$ ($P < 0.001$), respectively. In addition, an MTT assay demonstrated that preconditioning cells with 50 or 100 μM H_2O_2 attenuated the reduction of N2a cell viability induced by 600 μM H_2O_2 , compared with the non-preconditioned group ($P < 0.05$ and $P < 0.01$, respectively; Fig. 2), with 100 μM H_2O_2 most effective. Preconditioning with 20 μM H_2O_2 failed to significantly attenuate the reduction in cell viability induced by treatment with 600 μM H_2O_2 ($P > 0.05$; Fig. 2). Therefore, 100 μM H_2O_2 was selected for preconditioning in subsequent experiments.

H_2O_2 preconditioning decreases neuronal apoptosis, caspase-3 activity and 8-OHdG content. Following exposure of N2a cells to 600 μM H_2O_2 for 12 h, the percentage of apoptotic N2a cells increased significantly compared with the control (62.8 ± 5.2 vs. $6.5 \pm 0.5\%$; $P < 0.01$; Fig. 3). Preconditioning with 100 μM H_2O_2 for 90 min did not significantly alter the apoptotic rate compared with the control (9.5 ± 0.89 vs. $6.5 \pm 0.5\%$; $n = 5$; $P > 0.05$; Fig. 3); however, subsequent 600 μM H_2O_2 -induced apoptosis was significantly inhibited following preconditioning compared with the non-preconditioned group (33.8 ± 3.1 vs. $62.8 \pm 5.2\%$, respectively; $n = 5$; $P < 0.01$; Fig. 3).

The caspase 3 protein is a member of the cysteine-aspartic acid protease (caspase) family (17). Sequential activation of caspases serves a central role in the execution-phase of cell apoptosis, thus caspase-3 activity is a marker of cell apoptosis (18). Consistent with the results of flow cytometric analysis, caspase-3 activity was significantly decreased in N2a cells preconditioned with 100 μM H_2O_2 and exposed to 600 μM H_2O_2 compared with the non-preconditioned group ($P < 0.01$; Fig. 4).

8-OHdG is a marker of oxidative stress (19). The present study observed that 8-OHdG content was additionally significantly decreased in N2a cells preconditioned with 100 μM H_2O_2 and exposed to 600 μM H_2O_2 compared with the non-preconditioned group ($P < 0.01$; Fig. 5).

Effect of H_2O_2 preconditioning on ATM expression. The effect of 100 μM H_2O_2 preconditioning on ATM mRNA and protein expression levels was determined. Preconditioning of N2a cells

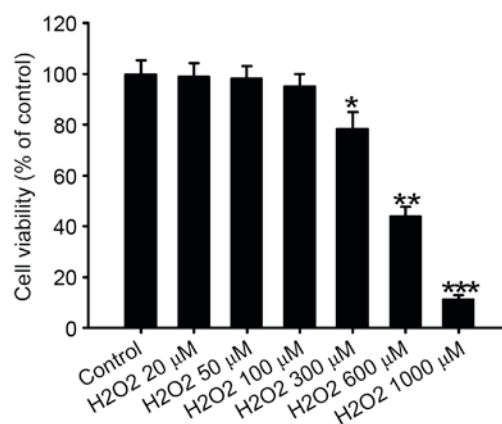


Figure 1. Effect of exposure to H_2O_2 on Neuro-2a cell viability. Data are expressed as the mean \pm standard error ($n = 5$). * $P < 0.05$, ** $P < 0.01$ and *** $P < 0.001$ vs. control.

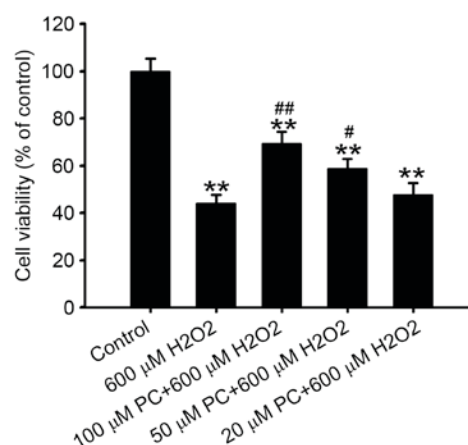


Figure 2. Effect of PC with H_2O_2 on Neuro-2a cell viability. Data are expressed as the mean \pm standard error ($n = 5$). ** $P < 0.01$ vs. control; # $P < 0.05$ and ## $P < 0.01$ vs. 600 μM H_2O_2 . PC, preconditioning.

with 100 μM H_2O_2 for 90 min significantly increased p-ATM protein expression levels compared with the control ($P < 0.01$; Fig. 6). Preconditioning with 100 μM H_2O_2 for 90 min, then 12 h later, increased the expression of ATM mRNA and protein when compared with the control ($P < 0.01$; Fig. 7A and B).

ATM inhibition or knockdown attenuates the protective effect of H_2O_2 preconditioning. To determine the involvement of ATM in H_2O_2 preconditioning, RNA interference (RNAi) with siRNA, and treatment with an ATM inhibitor, was performed. siRNA-mediated knockdown of ATM resulted in reduction of ATM protein expression compared with the untransfected control and scramble control groups ($P < 0.01$; Fig. 8). When N2a cells were incubated with 10 $\mu mol/l$ Ku55933 for 36 h or transfected with 50 nM control siRNA, the percentage of apoptotic cells was 8.0 ± 0.68 and $11.1 \pm 0.96\%$, respectively, and were not significantly different compared with the control group ($6.5 \pm 0.5\%$; $P > 0.05$; Fig. 3). However, the anti-apoptotic effect of preconditioning with 100 μM H_2O_2 was decreased by pretreatment with the ATM inhibitor Ku55933 or silencing of ATM with RNAi compared with the preconditioned group ($P < 0.01$ and $P < 0.01$, respectively; Fig. 3). In addition, the

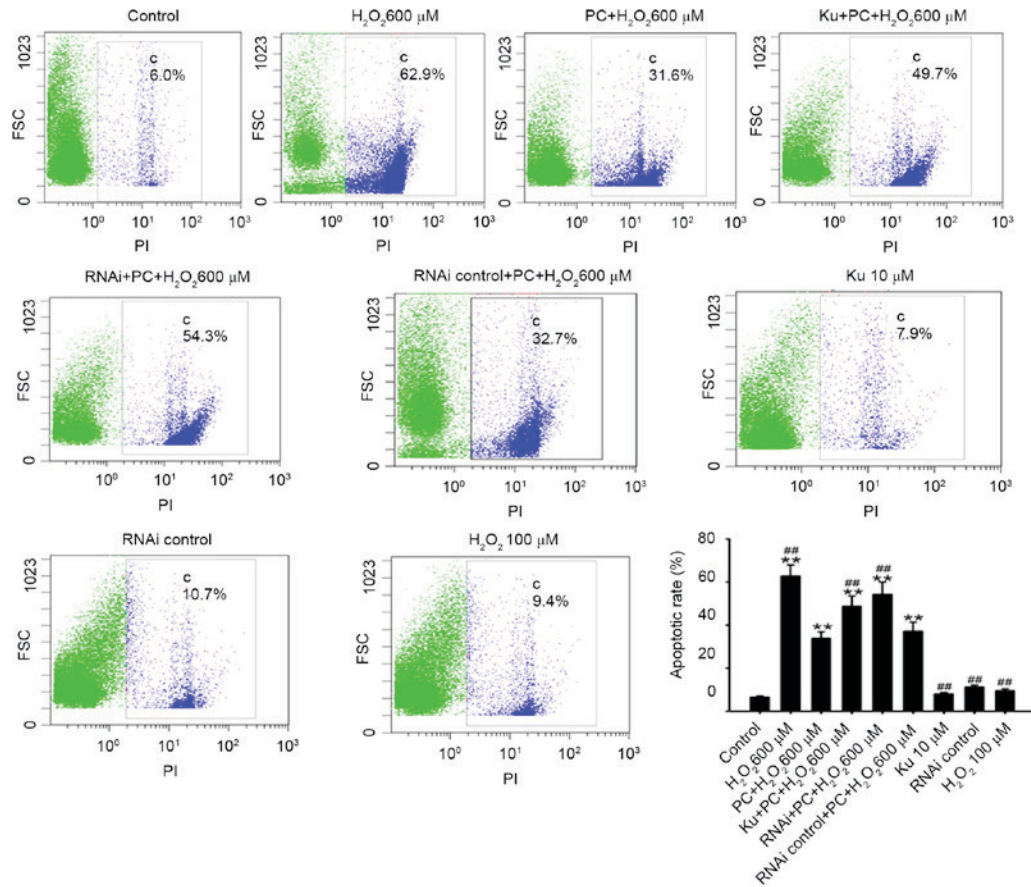


Figure 3. Effect of various treatments on apoptosis induced by 12 h exposure to 600 μM H_2O_2 in Neuro-2a cells, assessed by flow cytometry. Data are expressed as the mean \pm standard error ($n=5$). ** $P<0.01$ vs. control; ## $P<0.01$ vs. PC + 600 μM H_2O_2 . PI, propidium iodide; PC, preconditioned with 100 μM H_2O_2 ; Ku, Ku55933; RNAi, RNA interference with small interfering RNA; RNAi control, control small interfering RNA.

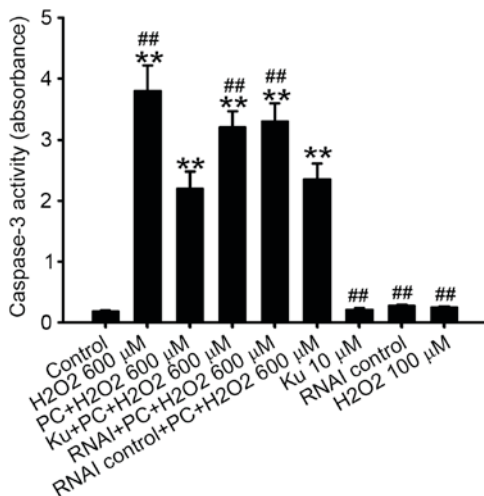


Figure 4. Effect of various treatments on caspase-3 activity in Neuro-2a cells following exposure to 600 μM H_2O_2 , as assessed using a colorimetric CaspACE kit. Data are expressed as the mean \pm standard error ($n=5$). ** $P<0.01$ vs. control; ## $P<0.01$ vs. PC + 600 μM H_2O_2 . PC, preconditioned with 100 μM H_2O_2 ; Ku, Ku55933; RNAi, RNA interference with small interfering RNA; RNAi control, control small interfering RNA.

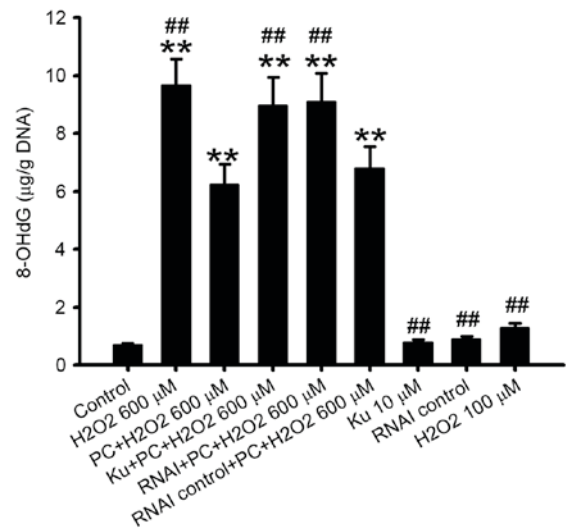


Figure 5. Effect of various treatments on 8-OHdG levels in Neuro-2a cells, as determined using a 8-OHdG ELISA assay. Data are expressed as the mean \pm standard error ($n=5$). ** $P<0.01$ vs. control; ## $P<0.01$ vs. PC + 600 μM H_2O_2 . 8-OHdG, 8-hydroxy-2'-deoxyguanosine; PC, preconditioned with 100 μM H_2O_2 ; Ku, Ku55933; RNAi, RNA interference with small interfering RNA; RNAi control, control small interfering RNA.

decreased caspase-3 activity observed following preconditioning with 100 μM H_2O_2 was inhibited by the pretreatment of cells with the ATM inhibitor Ku55933 or silencing of ATM with RNAi compared with the preconditioned group ($P<0.01$

and $P<0.01$, respectively; Fig. 4) and the decrease in 8-OHdG content observed following preconditioning with 100 μM H_2O_2 was also inhibited by pretreatment with the ATM inhibitor

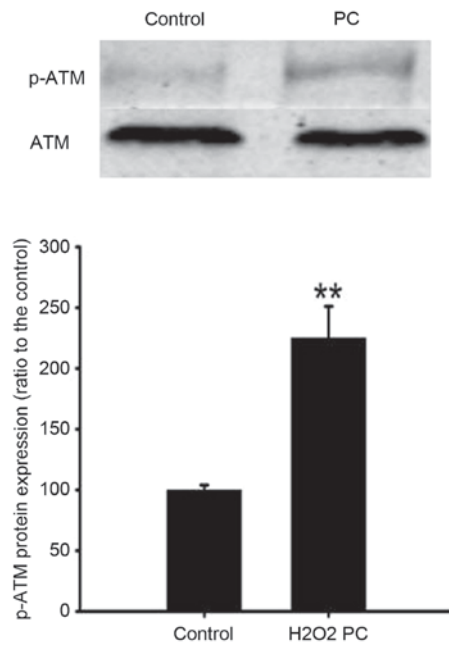


Figure 6. Effect of H_2O_2 preconditioning on p-ATM expression, as determined by western blot analysis. Data are expressed as the mean \pm standard error ($n=3-5$). ** $P<0.01$ vs. control. p-, phosphorylated; ATM, ataxia-telangiectasia mutated; PC, preconditioned with $100 \mu M H_2O_2$.

Ku55933 or silencing of ATM with RNAi compared with the preconditioned group ($P<0.01$ and $P<0.01$, respectively; Fig. 5).

Discussion

The results of the present study revealed that H_2O_2 preconditioning protects N2a cells against oxidative stress-induced injury, H_2O_2 preconditioning upregulates ATM mRNA and protein expression levels, and pretreatment with an ATM inhibitor or knockdown of ATM abrogates the protective effects of H_2O_2 preconditioning against lethal H_2O_2 -induced cell injury. This demonstrated that ATM may mediate the protective effects of H_2O_2 preconditioning.

Oxidative stress induced by ROS is a primary cause of ischemia/reperfusion injury; however, previous studies have reported that ROS generated from brief ischemia/reperfusion events triggers preconditioning-like protection. Brief exposure to exogenous oxygen species protected PC12 cells and neurons against subsequent serious oxidative stress injury via opening of surface K_{ATP} channels (20), increasing expression of Bcl-2 (1) and hypoxia-inducible factor-1 α protein (21), or enhancing the expression and functional activities of volume-activated chloride channels (22). The present study observed that H_2O_2 preconditioning protected against oxidative stress-induced injury in N2a cells, as assessed by MTT assays, flow cytometry, and analysis of caspase-3 activity and 8-OHdG content.

Although numerous previous studies have been performed, the cellular and molecular mechanisms underlying preconditioning remain to be fully clarified. A previous study reported that activation of ATM regulates cell redox homeostasis in various ways, including the enhancement of glucose-6-phosphate dehydrogenase activity, thereby increasing the

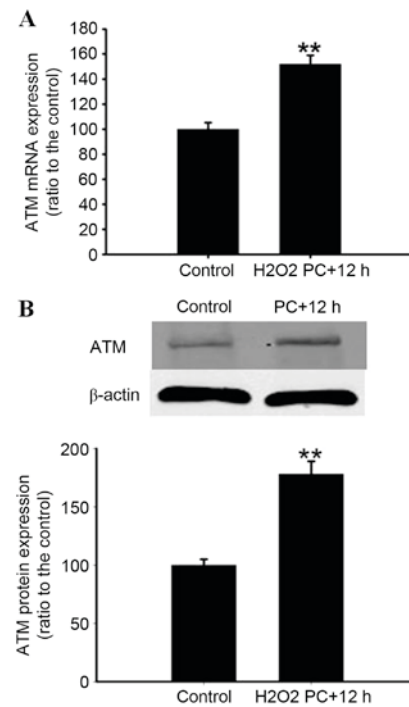


Figure 7. Effect of H_2O_2 preconditioning on (A) ATM mRNA and (B) protein expression levels. Data are expressed as the mean \pm standard error ($n=3-5$). ** $P<0.01$ vs. control. ATM, ataxia-telangiectasia mutated; PC, preconditioned with $100 \mu M H_2O_2$.

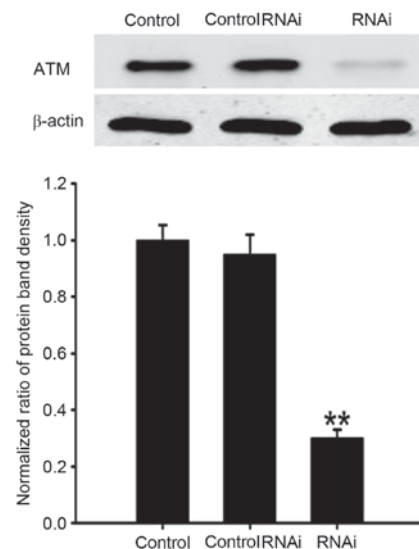


Figure 8. ATM protein expression levels are downregulated by RNAi. Data are expressed as the mean \pm standard error ($n=3$). ** $P<0.01$ vs. control. ATM, ataxia-telangiectasia mutated; RNAi, RNA interference with small interfering RNA; RNAi control, control small interfering RNA.

intracellular nicotinamide adenine dinucleotide phosphate and glutathione content significantly (10). ATM-deficient lymphoid stem cells exhibit mitochondrial dysfunction and a significant increase in ROS; exogenous ATM restores mitochondrial function and reduces the generation of ROS (23). ATM is additionally present in the peroxisomes, regulating catalase activity (24). Previous studies have reported that when PC12 cells or neurons were subjected to metabolic stress including

serum starvation, ATM regulated the insulin-associated signaling pathway and inhibited neuronal apoptosis (25,26). In addition, a previous study indicated that histone acetyltransferase 4 accumulates more readily in the nuclei of ATM-deficient neurons, and inhibits myocyte enhancer factor 2A/cyclic adenosine monophosphate response element binding-dependent transcription to promote neurodegeneration (27). Based on these findings, ATM is regarded as an essential endogenous protective protein against stress (4).

As the preconditioning process induces endogenous protective mechanisms, it was hypothesized that ATM may be involved in H₂O₂ preconditioning. Therefore, the effect of H₂O₂ preconditioning on the expression levels of ATM was measured. Notably, H₂O₂ preconditioning was observed to increase the protein expression levels of p-ATM, which indicated that H₂O₂ preconditioning activated ATM. Following H₂O₂ preconditioning for 12 h, ATM mRNA and protein expression levels increased, which supported this hypothesis. Additionally, the ATM inhibitor Ku55933, or knockdown of ATM using RNAi, attenuated the protective effect of H₂O₂ preconditioning against oxidative stress-induced injury. These data suggested that ATM is involved in H₂O₂ preconditioning.

In conclusion, the results of the present study demonstrated, to the best of our knowledge for the first time, that H₂O₂ preconditioning activates ATM and upregulates ATM mRNA and protein expression levels in N2a cells. Treatment with the ATM inhibitor, Ku55933, or silencing of ATM with RNAi attenuated the protective effect of H₂O₂ preconditioning in N2a cells. These results provide insight into the mechanisms underlying the involvement of ATM in H₂O₂ preconditioning. In addition, the present study highlights the potential of the ATM protein as a key therapeutic target for the prevention and treatment of ischemic brain damage.

Acknowledgements

The present study was supported by the National Nature Science Foundation of China (grant no. 81301057 to J.H.W. and grant no. 30971428 to D.F.W), the Foundation of Health and Family Planning Commission of Hubei province (grant no. WJ2015MB029 to D.F.W) and the Chenguang Plan of Wuhan Municipal Science and Technology Bureau (grant no. 2014070404010226 to J.L.).

References

1. Tang XQ, Feng JQ, Chen J, Chen PX, Zhi JL, Cui Y, Guo RX and Yu HM: Protection of oxidative preconditioning against apoptosis induced by H₂O₂ in PC12 cells: Mechanisms via MMP, ROS, and Bcl-2. *Brain Res* 1057: 57-64, 2005.
2. León OS, Menéndez S, Merino N, Castillo R, Sam S, Pérez L, Cruz E and Bocci V: Ozone oxidative preconditioning: A protection against cellular damage by free radicals. *Mediators Inflamm* 7: 289-294, 1998.
3. Shiloh Y: ATM and related protein kinases: Safeguarding genome integrity. *Nat Rev Cancer* 3: 155-168, 2003.
4. Bhatti S, Kozlov S, Farooqi AA, Naqi A, Lavin M and Khanna KK: ATM protein kinase: The linchpin of cellular defenses to stress. *Cell Mol Life Sci* 68: 2977-3006, 2011.
5. Kuang X, Yan M, Ajmo JM, Scofield VL, Stoica G and Wong PK: Activation of AMP-activated protein kinase in cerebella of Atm^{-/-} mice is attributable to accumulation of reactive oxygen species. *Biochem Biophys Res Commun* 418: 267-272, 2012.
6. Kamsler A, Daily D, Hochman A, Stern N, Shiloh Y, Rotman G and Barzilai A: Increased oxidative stress in ataxia telangiectasia evidenced by alterations in redox state of brains from Atm-deficient mice. *Cancer Res* 61: 1849-1854, 2001.
7. Kim TS, Kawaguchi M, Suzuki M, Jung CG, Asai K, Shibamoto Y, Lavin MF, Khanna KK and Miura Y: The ZFXH3 (ATBF1) transcription factor induces PDGFRB, which activates ATM in the cytoplasm to protect cerebellar neurons from oxidative stress. *Dis Model Mech* 3: 752-762, 2010.
8. Frappart PO and McKinnon PJ: Ataxia-telangiectasia and related diseases. *Neuromolecular Med* 8: 495-511, 2006.
9. Hoche F, Seidel K, Theis M, Vlaho S, Schubert R, Zielen S and Kieslich M: Neurodegeneration in ataxia telangiectasia: What is new? What is evident? *Neuropediatrics* 43: 119-129, 2012.
10. Cosentino C, Grieco D and Costanzo V: ATM activates the pentose phosphate pathway promoting anti-oxidant defence and DNA repair. *EMBO J* 30: 546-555, 2011.
11. Dobbin MM, Madabhushi R, Pan L, Chen Y, Kim D, Gao J, Ahanonu B, Pao PC, Qiu Y, Zhao Y and Tsai LH: SIRT1 collaborates with ATM and HDAC1 to maintain genomic stability in neurons. *Nat Neurosci* 16: 1008-1015, 2013.
12. Khanna KK, Lavin MF, Jackson SP and Mulhern TD: ATM, a central controller of cellular responses to DNA damage. *Cell Death Differ* 8: 1052-1065, 2001.
13. Ditch S and Paull TT: The ATM protein kinase and cellular redox signaling: Beyond the DNA damage response. *Trends Biochem Sci* 37: 15-22, 2012.
14. Li MJ, Wang WW, Chen SW, Shen Q and Min R: Radiation dose effect of DNA repair-related gene expression in mouse white blood cells. *Med Sci Monit* 17: BR290-BR297, 2011.
15. Li JZ, Wu JH, Yu SY, Shao QR and Dong XM: Inhibitory effects of paeoniflorin on lysophosphatidylcholine-induced inflammatory factor production in human umbilical vein endothelial cells. *Int J Mol Med* 31: 493-497, 2013.
16. Livak KJ and Schmittgen TD: Analysis of relative gene expression data using real-time quantitative PCR and the 2⁻(Delta Delta C(T)) Method. *Methods* 25: 402-408, 2001.
17. Alnemri ES, Livingston DJ, Nicholson DW, Salvesen G, Thornberry NA, Wong WW and Yuan J: Human ICE/CED-3 protease nomenclature. *Cell* 87: 171, 1996.
18. Ghavami S, Hashemi M, Ande SR, Yeganeh B, Xiao W, Eshraghi M, Bus CJ, Kadkhoda K, Wiehce E, Halayko AJ and Los M: Apoptosis and cancer: Mutations within caspase genes. *J Med Genet* 46: 497-510, 2009.
19. Zhang N, Komine-Kobayashi M, Tanaka R, Liu M, Mizuno Y and Urabe T: Edaravone reduces early accumulation of oxidative products and sequential inflammatory responses after transient focal ischemia in mice brain. *Stroke* 36: 2220-2225, 2005.
20. Tang XQ, Chen J, Tang EH, Feng JQ and Chen PX: Hydrogen peroxide preconditioning protects PC12 cells against apoptosis induced by oxidative stress. *Sheng Li Xue Bao* 57: 211-216, 2005.
21. Chang S, Jiang X, Zhao C, Lee C and Ferriero DM: Exogenous low dose hydrogen peroxide increases hypoxia-inducible factor-1alpha protein expression and induces preconditioning protection against ischemia in primary cortical neurons. *Neurosci Lett* 441: 134-138, 2008.
22. Zhu L, Zuo W, Yang H, Zhang H, Luo H, Ye D, Lin X, Mao J, Feng J, Chen L and Wang L: Involvement of volume-activated chloride channels in H₂O₂ preconditioning against oxidant-induced injury through modulating cell volume regulation mechanisms and membrane permeability in PC12 cells. *Mol Neurobiol* 48: 205-216, 2013.
23. Ambrose M, Goldstine JV and Gatti RA: Intrinsic mitochondrial dysfunction in ATM-deficient lymphoblastoid cells. *Hum Mol Genet* 16: 2154-2164, 2007.
24. Watters D, Kedar P, Spring K, Bjorkman J, Chen P, Gatei M, Birrell G, Garrone B, Srinivasa P, Crane DI and Lavin MF: Localization of a portion of extranuclear ATM to peroxisomes. *J Biol Chem* 274: 34277-34282, 1999.
25. Li Y, Xiong H and Yang DQ: Functional switching of ATM: Sensor of DNA damage in proliferating cells and mediator of Akt survival signal in post-mitotic human neuron-like cells. *Chin J Cancer* 31: 364-372, 2012.
26. Yang DQ, Halaby MJ, Li Y, Hibma JC and Burn P: Cytoplasmic ATM protein kinase: An emerging therapeutic target for diabetes, cancer and neuronal degeneration. *Drug Discov Today* 16: 332-338, 2011.
27. Li J, Chen J, Ricupero CL, Hart RP, Schwartz MS, Kusnecov A and Herrup K: Nuclear accumulation of HDAC4 in ATM deficiency promotes neurodegeneration in ataxia telangiectasia. *Nat Med* 18: 783-790, 2012.